

Mixture-of-Experts with Gradient Conflict-Driven Subspace Topology Pruning for Emergent Modularity

Yuxing Gan¹ and Ziyu Lei^{2,*}

¹Independent Researcher

²Huazhong University of Science and Technology

December 24, 2025

Abstract

Mixture-of-Experts (MoE) architectures achieve parameter efficiency through conditional computation, yet contemporary designs suffer from two fundamental limitations: *structural parameter isolation* that causes catastrophic forgetting, and *instruction-overfitting* that degrades performance in instruction-free scenarios. We propose CDSP-MoE (Conflict-Driven Subspace Pruning MoE), a framework that addresses these issues through a paradigm shift from isolated expert containers to *dynamic expert instantiation within a shared physical subspace*. Grounded in the Universal Weight Subspace Hypothesis, CDSP-MoE maintains a super-complete parameter backbone where logical experts are carved out via learnable topology masks. Unlike prior work that uses gradient conflict for token reassignment or optimization surgery, we leverage it as a *structural supervisory signal*: a Lagged Gradient Game penalizes interfering connections in the shared manifold, enabling the topology to spontaneously prune conflicting pathways and evolve interpretable modular structures. Experimental results demonstrate that CDSP-MoE achieves robust content-driven routing without human-defined task labels, maintaining semantic specialization even under strict blind inference protocols where explicit instructions are absent. Code is available at: <https://github.com/konodiodaaaaa1/Conflict-Driven-Subspace-Pruning-Mixture-of-Experts>

Keywords: Mixture-of-Experts, Gradient Conflict, Subspace Topology Pruning, Dynamic Expert Instantiation, Emergent Modularity, Instruction-Free Routing, Shared Parameter Manifold, Lagged Gradient Game, Structural Evolution, Multi-Task Learning.

1 Introduction

The scaling of Large Language Models (LLMs) has been profoundly catalyzed by the Mixture-of-Experts (MoE) paradigm. By conditionally activating a subset of parameters, architectures like GShard [5] and Switch Transformer [2] have broken the dense scaling barrier. Recent advancements, such as DeepSeek-MoE [1], have further optimized this via fine-grained expert segmentation and shared-expert mechanisms, achieving remarkable efficiency.

However, a fundamental limitation persists in these state-of-the-art architectures: *structural parameter isolation*. In standard MoE designs, routed experts are instantiated as disjoint, independent tensors with no physical connectivity. To utilize these isolated experts, routers heavily rely on heuristic auxiliary losses to enforce load balancing. This leads to two critical failures:

- **Memory Overwrite & Catastrophic Forgetting:** The pursuit of load balancing often forces semantically unrelated tokens to update the same expert. Since experts are isolated containers without orthogonal subspaces, new gradient updates inadvertently overwrite

previously learned knowledge, creating a “tug-of-war” dynamic that degrades performance in multi-task continuous learning.

- **Knowledge Fragmentation & Hallucination:** The strict isolation of expert parameters severs the intrinsic semantic links between concepts. While shared experts provide a partial remedy, the routed experts remain functionally siloed, leading to fragmented knowledge representation that is prone to hallucinations when synthesizing complex information.

To address these limitations, we propose Mixture-of-Experts with Conflict-Driven Subspace Pruning (CDSP-MoE). Moving beyond the paradigm of isolated parameter containers, we ground our framework in the *Universal Weight Subspace Hypothesis* [3], which posits that diverse tasks can be solved by varying combinations of a shared, low-rank basis. In CDSP-MoE, logical experts are no longer disjoint tensors but dynamic *instantiations* carved out from a super-complete physical backbone via topology-aware masking.

The core of our methodology is the Lagged Gradient Game, a mechanism inspired by multi-task gradient surgery [8]. Instead of treating gradient conflict as optimization noise to be suppressed, we leverage it as a structural supervisory signal. By monitoring the cosine similarity of gradients between experts on the shared backbone, CDSP-MoE penalizes connections that cause interference. This forces the topology to spontaneously prune conflicting pathways, evolving a modular structure where experts specialize not by forced instruction IDs, but by minimizing physical interference.

Our main contributions are summarized as follows:

- **Identification of Structural Isolation:** We identify that the parameter isolation in standard MoEs causes memory overwrite and hallucination, limiting their effectiveness in instruction-free routing.
- **Conflict-Driven Topology Evolution:** We propose CDSP-MoE, which utilizes a lagged gradient game to evolve expert modularity from a shared physical subspace without human-defined labels.
- **Robust Instruction-Free Performance:** Extensive experiments show that CDSP-MoE achieves superior zero-shot routing accuracy and interpretability compared to DeepSeek-MoE and LoRA baselines under blind inference protocols.

2 Related Work

2.1 Sparse Mixture-of-Experts

The concept of conditional computation was popularized by the Sparsely-Gated MoE [6], which introduced a noisy $top-k$ gating mechanism. Subsequent works like GShard [5] and Switch Transformer [2] focused on simplifying routing logic. More recently, DeepSeek-MoE [1] introduced fine-grained expert segmentation to enhance specialization.

Alternative Routing Strategies. To address the load imbalance issue in $top-k$ routing, Expert Choice Routing [10] inverts the mechanism by allowing experts to select the $top-k$ tokens, thereby enforcing perfect capacity utilization. However, this relies on fixed capacity constraints which can drop critical information. CDSP-MoE differs fundamentally: we abandon forced load balancing entirely. Instead of optimizing for server capacity, we use *conflict-driven pruning* to optimize for semantic interference, allowing expert utilization to be governed solely by physical compatibility.

2.2 Subspace Learning and LoRA

Our work is grounded in the Universal Weight Subspace Hypothesis [3]. Low-Rank Adaptation (LoRA) [4] exploits this by training low-rank matrices.

Adaptive Pruning. Our approach shares conceptual roots with AdaLoRA [9], which adaptively allocates parameter budgets by pruning singular values based on importance scores. While AdaLoRA optimizes the rank of static matrices for a specific dataset, CDSP-MoE operates on a shared physical manifold to perform *instance-wise* dynamic instantiation. This allows our model to reconfigure its effective topology on-the-fly for every token, rather than settling on a single static pruned structure.

2.3 Gradient Conflict in Multi-Task Learning

Gradient conflict arises when different tasks generate opposing parameter update directions, degrading multi-task optimization. Methods like PCGrad [8] address this through *gradient surgery*, projecting conflicting gradients to preserve task-specific directions during optimization.

Recent work has explored gradient conflict specifically within MoE architectures. STGC [7] identifies token-level gradient conflicts within each expert and introduces a conflict elimination loss to *reassign conflicting tokens to alternative experts*. While STGC improves routing decisions in vision-language models, it operates within the conventional MoE paradigm of largely isolated expert parameters: gradient conflict informs *which tokens go to which expert*, but the physical structure of experts remains architecturally fixed and independently parameterized.

Instead of using conflict to optimize routing over a fixed architecture, we use gradient conflict as a *discovery signal for structural pruning*. In our framework, experts are not isolated parameter containers but dynamic instantiations from a shared physical subspace. The Lagged Gradient Game monitors conflicts *within this shared manifold* and penalizes topological connections that cause interference. This induces an effective architectural evolution: conflicting pathways are pruned, and modular structures emerge at the level of functional topology, without pre-defined expert boundaries. Where STGC asks “which expert should process this token?”, CDSP-MoE asks “which physical dimensions should constitute each expert?” This architectural-level approach enables CDSP-MoE to achieve emergent specialization purely from physical compatibility, yielding robust instruction-free routing that persists even when task identifiers are completely absent.

3 Methodology

3.1 Framework Overview

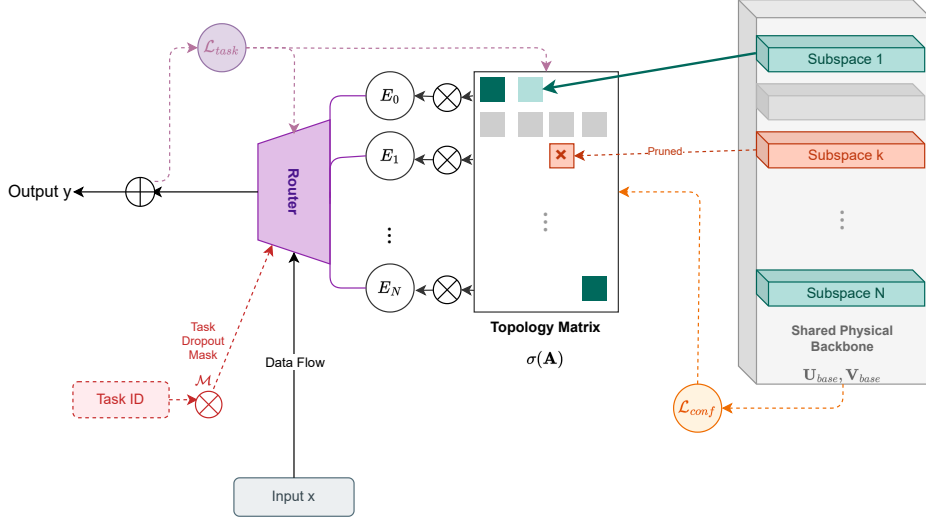


Figure 1: The CDSP-MoE Framework.

The overall architecture of CDSP-MoE is illustrated in Figure 1. Diverging from traditional MoEs that route inputs to isolated, static parameter containers, CDSP-MoE functions as a dynamic, three-layered evolutionary system:

1. **Physical Subspace Backbone (Bottom):** A super-complete, shared parameter manifold defined by U_{base} and V_{base} constituted by orthogonal projection matrices, serving as the universal substrate for feature extraction.
2. **Topology-Aware Instantiation (Middle):** A learnable topology matrix $\sigma(\mathbf{A})$ that acts as a soft-adjacency graph, dynamically instantiating logical experts (denoted as E_0, \dots, E_N) by masking (\otimes) specific physical subspaces based on router cues.
3. **Lagged Gradient Game (Feedback):** A dual-loop optimization mechanism where the task loss \mathcal{L}_{task} updates parameters for functional accuracy, while a separate conflict loss \mathcal{L}_{conf} serves as a negative feedback signal to prune interfering connections.

The following subsections detail the mathematical formulation of these components.

3.2 Physical Subspace Backbone

Standard MoE architectures maintain N discrete sets of parameters $\{\theta_1, \dots, \theta_N\}$, leading to structural isolation. In contrast, CDSP-MoE employs a Super-Complete Shared Parameter Space. We define the physical backbone Θ_{base} as a pair of orthogonal projection matrices:

$$\mathbf{U}_{base} \in \mathbb{R}^{D_{model} \times D_{base}}, \quad \mathbf{V}_{base} \in \mathbb{R}^{D_{base} \times D_{model}} \quad (1)$$

where D_{base} is the dimension of the shared subspace, typically set to $D_{base} \gg D_{model}$ (e.g., $4 \times D_{model}$) to satisfy the over-parameterization requirement for diverse feature extraction.

To provide a warm-start for the evolutionary process, we introduce a fixed Physical Initial Partition matrix $\mathbf{\Pi} \in \{0, 1\}^{N \times D_{base}}$. We employ a block-diagonal initialization strategy where each logical expert i is initially assigned a dedicated contiguous slice of the backbone:

$$\mathbf{\Pi}_{i,k} = \begin{cases} 1 & \text{if } \lfloor k/B \rfloor = i \\ 0 & \text{otherwise} \end{cases} \quad (2)$$

where $B = D_{base}/N$ is the block size. This partition serves as a reference coordinate system, not a hard constraint.

3.3 Topology-Aware Dynamic Instantiation

The logical structure of CDSP-MoE is defined by a learnable Topology Matrix $\mathbf{A} \in \mathbb{R}^{N \times N}$, representing a weighted directed graph between logical experts and physical partitions. The entry \mathbf{A}_{ij} denotes the connectivity strength of logical expert i to the physical partition initially belonging to expert j .

Structural Initialization. To ensure stability while allowing structural plasticity, we adopt a *Biased Weak-Connection* initialization strategy:

$$\mathbf{A}_{ij} \leftarrow \begin{cases} 1.0 & \text{if } i = j \quad (\text{Self-Preservation}) \\ 0.1 + \epsilon & \text{if } i \neq j \quad (\text{Weak Cross-Link}) \end{cases} \quad (3)$$

where $\epsilon \sim \mathcal{N}(0, 0.01)$. This setup guarantees that experts possess functional autonomy at initialization while maintaining weak global connectivity for gradient exploration.

Control Force Projection. The effective activation of physical dimensions is determined by the Control Force vector $\mathbf{I}_i \in \mathbb{R}^{D_{base}}$. For logical expert i , this is computed as the linear combination of the topology weights and the physical partition map:

$$\mathbf{I}_i = \sigma(\mathbf{A}_{i,:}) \cdot \mathbf{\Pi} \quad (4)$$

where $\sigma(\cdot)$ is the sigmoid function. $\mathbf{I}_{i,k}$ thus represents the net influence of logical expert i on the k -th physical dimension in the shared backbone.

3.4 Forward Dynamics: Subspace Addressing and Computation

Once the router selects a set of active logical experts $\mathcal{E} = \text{TopK}(G(x))$, the system must physically instantiate these experts from the shared backbone. This process involves three distinct phases: subspace addressing, sparse execution, and gradient bridging.

Subspace Addressing via Square Root Scaling. Unlike standard MoEs that retrieve discrete parameter blocks, CDSP-MoE dynamically assembles experts. For each active expert $i \in \mathcal{E}$, we determine its physical footprint by selecting the top- r dimensions from the control force vector \mathbf{I}_i . The active index set \mathcal{S}_i is defined as:

$$\mathcal{S}_i = \text{argtop}_r(\mathbf{I}_i), \quad \text{where } \mathbf{I}_i = \sigma(\mathbf{A}_{i,:}) \cdot \mathbf{\Pi} \quad (5)$$

To balance the trade-off between expert specialization and parameter capacity, we introduce a **Square Root Scaling Law** for the rank quota r :

$$r = \left\lfloor \frac{D_{base}}{\sqrt{N}} \right\rfloor \quad (6)$$

This scaling ensures that as the number of experts N increases, the subspace assigned to each expert becomes more sparse, enforcing stronger specialization while maintaining a constant total memory budget for the active parameters.

Sparse Computation. The forward computation is executed exclusively on the selected physical dimensions. Let $\mathbf{U}_{base}[\mathcal{S}_i]$ and $\mathbf{V}_{base}[\mathcal{S}_i]$ denote the sub-matrices of the backbone corresponding to the indices in \mathcal{S}_i . The raw output of expert i is computed as a low-rank projection:

$$y_{raw}^{(i)} = \text{SiLU}(x \cdot \mathbf{U}_{base}[\mathcal{S}_i]) \cdot \mathbf{V}_{base}[\mathcal{S}_i]^T \quad (7)$$

This operation is mathematically equivalent to a dense layer but is computationally sparse, as only r columns of the backbone are accessed from memory.

The Differentiable Gradient Bridge. A critical challenge in dynamic pruning is that the discrete index selection operation (argtop_r) is non-differentiable, blocking the flow of gradients from the task loss \mathcal{L}_{task} back to the topology matrix \mathbf{A} .

To resolve this, we introduce a **Strength Modulation** factor m_i , which acts as a differentiable bridge. We define m_i as the average activation strength of the selected subspace:

$$m_i = \frac{1}{r} \sum_{k \in \mathcal{S}_i} \mathbf{I}_{i,k} \quad (8)$$

The final output of expert i is modulated by this factor:

$$y_{final}^{(i)} = G(x)_i \cdot m_i \cdot y_{raw}^{(i)} \quad (9)$$

Mechanism Analysis: This modulation creates a valid gradient path. During backpropagation, the gradient $\frac{\partial \mathcal{L}}{\partial m_i}$ is non-zero, allowing error signals to propagate to $\mathbf{I}_{i,k}$ and subsequently to \mathbf{A}_{ij} .

- If a selected subspace \mathcal{S}_i contributes to reducing the loss, the gradient descent will increase m_i , thereby strengthening the topological connections \mathbf{A} pointing to these physical dimensions.
- Conversely, if the subspace is ineffective, the connection strength is suppressed.

This mechanism effectively creates a "soft" relaxation of the hard selection process, enabling end-to-end learning of the topology.

3.5 Perceptive Routing with Adversarial Masking

A critical failure mode in multi-task MoEs is *shortcut learning*, where the router overfits to explicit task identifiers (Task IDs) or prompt templates, ignoring the intrinsic semantics of the input content x . To enable robust instruction-free routing, we introduce an Adversarial Task Masking mechanism.

Input Fusion. The router input h_{in} is a fusion of the content representation and a potentially masked task embedding. To prevent the magnitude of token features from biasing the routing decision, we first normalize the input:

$$h_{in} = [\text{LayerNorm}(x) \oplus \mathbf{v}_{task}] \quad (10)$$

where \oplus denotes concatenation.

Adversarial Masking. During training, we view the Task ID not as a ground-truth label, but as a weak hint that should be gradually discarded. We define the effective task embedding \mathbf{v}_{task} using a stochastic mask \mathcal{M} :

$$\mathbf{v}_{task} = \mathcal{M} \cdot \text{Embed}(t), \quad \mathcal{M} \sim \text{Bernoulli}(1 - p_{drop}) \quad (11)$$

where p_{drop} is the masking probability.

- When $\mathcal{M} = 1$, the router sees the task ID (standard supervision).
- When $\mathcal{M} = 0$, the router is forced to infer the appropriate expert solely from the content x (blind inference).

By setting a high p_{drop} (e.g., $0.5 \rightarrow 0.9$) during training, we simulate a “blind” environment, forcing the router to uncover the latent alignment between semantic features and expert functionalities.

Gating Decision. The gating scores are then computed using a standard softmax over the fused representation:

$$G(x) = \text{Softmax}(\mathbf{W}_g \cdot h_{in}) \quad (12)$$

We select the top- k logical experts $\mathcal{E} = \text{TopK}(G(x))$ for the subsequent dynamic instantiation.

3.6 Gradient Conflict Optimization

The core novelty of CDSP-MoE is utilizing gradient conflict not as an optimization hurdle, but as a structural discovery signal. We formulate this as a *Lagged Gradient Game*.

Lagged Gradient Sampling. Directly computing gradient interference during the forward pass is computationally prohibitive. Instead, we employ a temporal decoupling strategy. Let $\mathcal{L}_{task}^{(t)}$ be the task loss at step t . During backpropagation, we capture the gradients of the physical backbone parameters Θ_{base} attributed to each active expert i :

$$\mathbf{g}_i^{(t)} = \nabla_{\Theta_{base}} \mathcal{L}_{task}^{(t)} \Big|_{\text{via expert } i} \quad (13)$$

To avoid overhead, these gradients are detached and stored. In step $t + 1$, we use the gradients $\mathbf{g}^{(t)}$ as "lagged signals" to optimize the topology.

Spatial Conflict Metric. Conflict only occurs when two experts i and j attempt to update the *same* physical parameters in *opposite* directions. We define the physical intersection set as $\mathcal{K}_{ij} = \mathcal{S}_i \cap \mathcal{S}_j$. If $\mathcal{K}_{ij} = \emptyset$, the conflict is zero. Otherwise, we calculate the cosine similarity strictly within this intersection:

$$\text{sim}(\mathbf{g}_i, \mathbf{g}_j) = \frac{\mathbf{g}_i[\mathcal{K}_{ij}] \cdot \mathbf{g}_j[\mathcal{K}_{ij}]}{\|\mathbf{g}_i[\mathcal{K}_{ij}]\| \|\mathbf{g}_j[\mathcal{K}_{ij}]\| + \epsilon} \quad (14)$$

We are interested only in destructive interference (negative similarity). The Conflict Score is defined as:

$$\mathcal{C}_{ij} = \text{ReLU}(-\text{sim}(\mathbf{g}_i, \mathbf{g}_j)) \quad (15)$$

This acts as a repulsive force: the more two experts fight for the same subspace, the higher the penalty.

Structural Evolution and Gradient Flow. The total objective function combines the task loss with the structural conflict penalty:

$$\mathcal{L}_{total} = \mathcal{L}_{task} + \lambda_{conf} \sum_{i \neq j} \underbrace{\sigma(\mathbf{A}_{ij}) \cdot \mathcal{C}_{ij}}_{\text{Conflict Loss}} + \lambda_{reg} \|\mathbf{A}\|_1 \quad (16)$$

Analysis of Gradient Flow: The optimization dynamics can be decomposed into two orthogonal pathways:

1. **Subspace Learning** ($\nabla_{\Theta} \mathcal{L}_{task}$): The task loss updates the values of the physical backbone Θ_{base} , enabling feature extraction.
2. **Topology Pruning** ($\nabla_{\mathbf{A}} \mathcal{L}_{conf}$): The conflict loss generates gradients w.r.t the topology matrix \mathbf{A} . specifically:

$$\frac{\partial \mathcal{L}_{conf}}{\partial \mathbf{A}_{ij}} = \sigma'(\mathbf{A}_{ij}) \cdot \mathcal{C}_{ij} \quad (17)$$

This derivation reveals the pruning mechanism: if expert i has a strong connection to a subspace (high $\sigma(\mathbf{A}_{ij})$) that causes high conflict (\mathcal{C}_{ij}), the gradient $\frac{\partial \mathcal{L}_{conf}}{\partial \mathbf{A}_{ij}}$ becomes large and positive. Gradient descent then decreases \mathbf{A}_{ij} , effectively ‘‘cutting’’ the wire to that subspace. This forces the expert to migrate to a conflict-free region of the backbone.

3.7 Optimization Strategy

To stabilize this co-evolutionary process, we employ a Two-Speed Optimization schedule:

- **Physical Parameters** (Θ_{base}): Optimized with a standard learning rate η and weight decay. This ensures stable feature accumulation.
- **Topology Parameters** (\mathbf{A}): Optimized with a higher learning rate (e.g., 10η) but *zero weight decay*.

The higher rate for \mathbf{A} allows the topology to adapt rapidly to the detected conflicts ("fast plasticity"), while the physical backbone consolidates knowledge slowly ("slow stability").

4 Experiments

Our experimental evaluation is designed not merely to chase marginal accuracy gains, but to verify the central hypothesis of this paper: that exitconflict-driven pruning can induce emergent modularity without human-defined semantic labels. We conduct controlled experiments in a heterogeneous multi-task environment to compare the structural evolution of CDSP-MoE against standard baselines.

4.1 Experimental Setup

Heterogeneous Multi-Task Environment. To simulate a scenario with varying levels of semantic conflict and synergy, we construct a mixed task stream comprising three classic datasets:

- **Task 0 (MNIST):** Handwritten digit recognition (0-9). Represents simple, sparse symbolic patterns.
- **Task 1 (KMNIST):** Kuzushiji (cursive Japanese) characters (10 classes). Represents complex symbolic patterns with high stroke density.
- **Task 2 (Fashion-MNIST):** Clothing article recognition (10 classes). Represents dense, texture-rich object imagery.

Hypothetically, an intelligent router should spontaneously group the symbolic tasks (MNIST and KMNIST) while isolating the object recognition task (Fashion-MNIST) due to their conflicting feature distributions. All inputs are flattened to $1 \times 28 \times 28$ grayscale patches.

Model Configurations. We compare CDSP-MoE against a standard MoE baseline. To ensure a fair comparison focused on structural efficiency rather than capacity, we enforce a strict `exitIso-Parameter Constraint`:

- **Baseline (Standard MoE):** A standard Top-2 gating network with $N = 8$ independent experts. Each expert has a dedicated weight matrix of dimension $d = 32$. The router utilizes explicit Task IDs during training and relies on standard auxiliary load-balancing losses.
- **Ours (CDSP-MoE):** Configured with $N = 8$ logical experts sharing a single super-complete physical backbone ($D_{base} = 256$). The total parameter count is aligned with the baseline ($\approx 32k$). The router is trained with Task Dropout ($p = 0.1$) to encourage content dependency.

Training Protocol. Models are trained using the AdamW optimizer. A key detail is the Two-Speed Learning Rate: the physical parameters are trained at $\eta = 5e - 3$, while the topology matrix \mathbf{A} is evolved at 10η ($5e - 2$). This differential rate is critical for allowing the structure to evolve faster than the accumulation of weight knowledge ("Evolutionary Tax"), ensuring that connections are pruned before they overfit to noise.

4.2 Evaluation Philosophy: From Identity to Content

Traditional MoE evaluations often prioritize peak accuracy on known tasks. However, this metric fails to capture whether the model has truly learned to route based on semantics or is simply memorizing Task ID mappings ("Identity Politics"). We propose a more rigorous evaluation protocol based on two core logics:

1. **Blind Inference (Instruction-Free):** Can the model correctly route inputs when the Task ID is stripped (i.e., set to `None` or a zero vector)? A content-driven model should maintain routing consistency, while an ID-driven model is expected to collapse to random guessing or a default expert.
2. **Emergent Clustering:** Without manual instruction, does the model spontaneously discover that MNIST and KMNIST are semantically closer to each other than to Fashion-MNIST? We verify this by analyzing the overlap in expert utilization heatmaps.

4.3 Results and Analysis

We present the comparative analysis of the proposed CDSP-MoE against the Standard MoE Baseline across three distinct experiments.

4.3.1 Experiment I: Emergent Modularity in CDSP-MoE

In this experiment, we analyze the structural evolution of CDSP-MoE. We visualize the internal topology matrix, the routing distribution over training epochs, and the blind inference behavior.

Topology Evolution: From Chaos to Oligarchy. Figure 2 visualizes the sigmoid-activated topology matrix $\sigma(\mathbf{A})$ across training epochs.

- **Initialization (Epoch 0):** All experts start with weak, uniform cross-connections, representing a dense but low-magnitude potential.

- **Pruning and Specialization (Epoch 9):** Under the pressure of the conflict loss \mathcal{L}_{conf} and L1 regularization, a clear "oligarchic" structure emerges. As shown in Figure 2(b), only a subset of experts (E5, E7, E2, E0) maintain high diagonal weights (> 0.8), while others (E1, E3, E4, E6) are effectively marginalized. This confirms that CDSP-MoE spontaneously discovers the minimal effective parameter set.

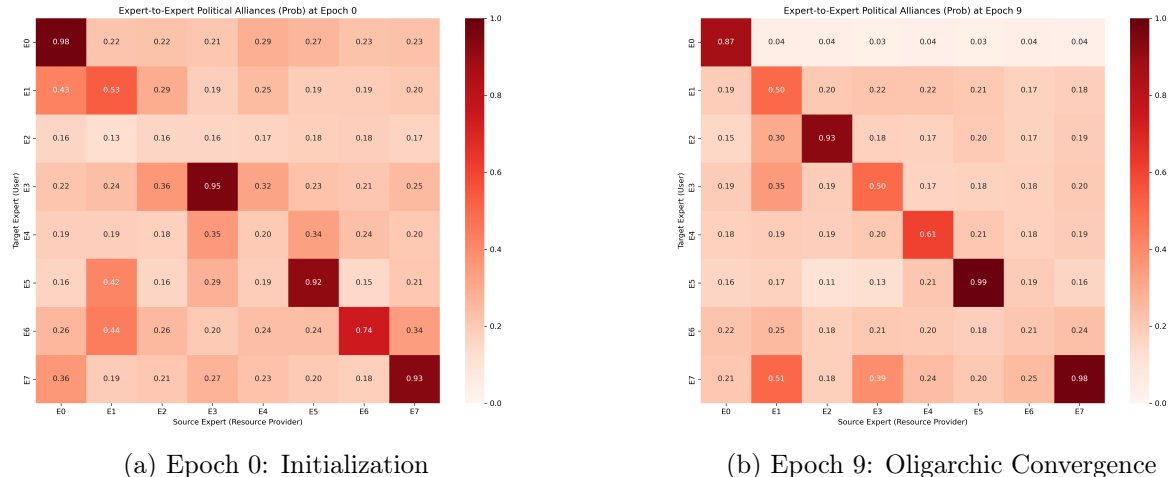


Figure 2: Evolution of the topology matrix $\sigma(\mathbf{A})$ across training epochs.

Routing Dynamics: From Complexity Bias to Semantic Alignment. The routing heatmaps in Figure 3 reveal a two-stage evolution.

- **Stage 1: Complexity Bias (Epoch 2).** Initially, the router groups KMNIST (Task 1) and Fashion-MNIST (Task 2) together, routing them primarily to Experts E0 and E2. This suggests an initial bias towards visual complexity (high-frequency patterns) rather than semantics.
- **Stage 2: Semantic Convergence (Epoch 9).** As the conflict game progresses, the model spontaneously realigns KMNIST with MNIST, routing both "symbolic" tasks to the E0/E5 cluster, while Fashion-MNIST migrates to a dedicated expert E7. This proves that the model successfully disentangles "symbolic" concepts from "object" concepts.

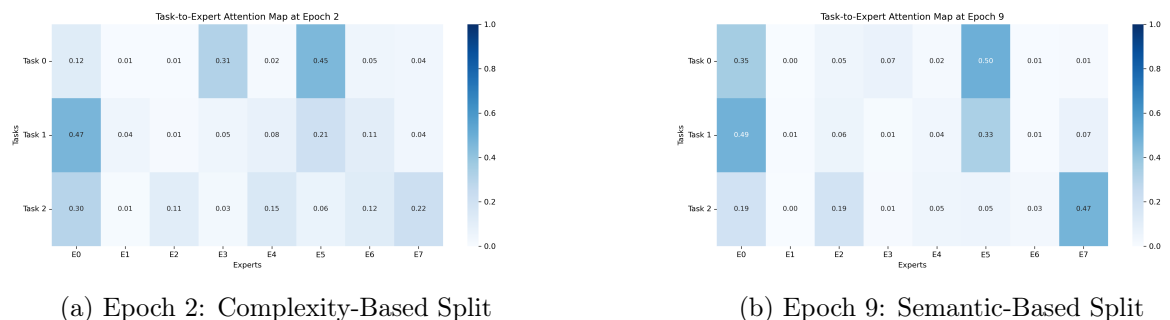


Figure 3: Comparison of expert utilization heatmaps between Epoch 2 and Epoch 9.

Blind Test: Robustness and Uncertainty Drift. Figure 4 presents the routing behavior when Task IDs are forcibly removed (Input None).

- **Semantic Robustness:** The primary semantic boundary remains intact. The "Symbolic Cluster" (Real T0 and T1) is still dominantly routed to E0 and E5, while the "Object Task" (Real T2) maintains its distinct preference for E7.

- **Uncertainty Drift in E0:** We observe a notable nuance: under blind inference, E0 receives a moderate portion of Task 2 traffic (unlike the strict zero in the standard mode). This suggests that E0 acts as a *foundational expert*, encoding low-level visual primitives, serving as a fallback option when explicit instruction signals are lost.

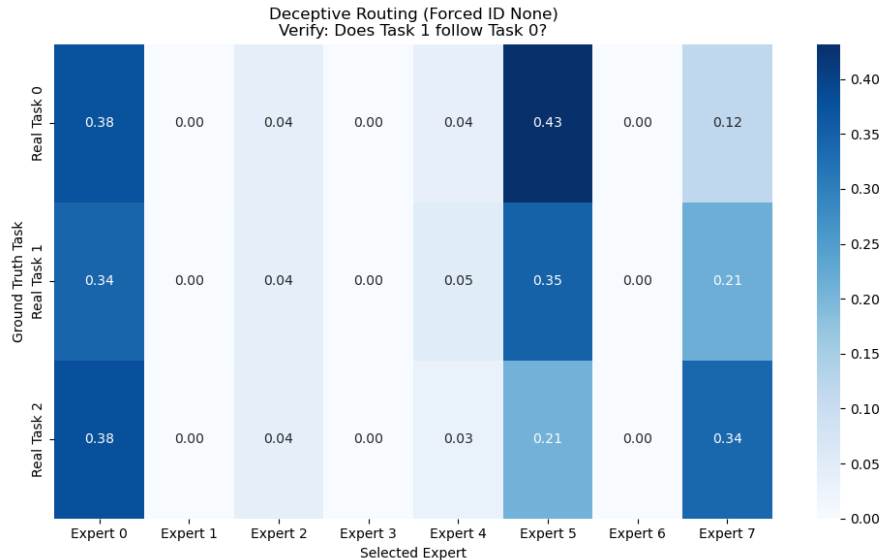


Figure 4: Routing distribution of CDSP-MoE under blind inference (Task ID = None).

4.3.2 Experiment II: Instruction Overfitting in Standard Baselines

To validate that the emergent modularity observed in CDSP-MoE is not a trivial result of data statistics, we evaluate the Standard MoE Baseline (Iso-Parameter) under the same protocols.

Training State: The Lookup Table Illusion. Figure 5 illustrates the routing distribution of the Baseline at Epoch 9 with explicit Task IDs.

- **Superficial Efficiency:** The model establishes a sharp division of labor (e.g., Task 2 to Expert 2).
- **The Lookup Table Mechanism:** While this appears effective, it reveals a reliance on "shortcut learning." The router learns a simple linear mapping from $ID \rightarrow Expert$, bypassing the need to analyze the visual features of the input.

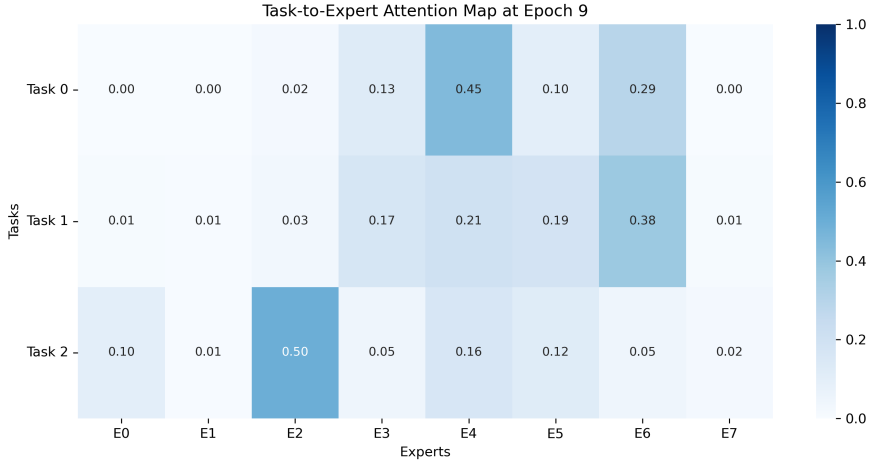


Figure 5: Routing distribution of the Standard MoE Baseline in the training state.

Blind Inference: Static Mode Collapse. The fragility of the baseline is exposed in the blind inference test (Figure 6), where Task IDs are removed.

- **Feature Blindness:** The Baseline fails to distinguish between symbolic inputs (Real T0) and object inputs (Real T2). The routing distributions for all three tasks are nearly identical (Pearson correlation ≈ 1.0).
- **Loss of Specialized Knowledge:** Expert 2, the "Clothing Expert" during training, is abandoned. The router defaults to experts with the highest global frequency bias (E4 and E6), demonstrating a complete lack of content-driven decision making.

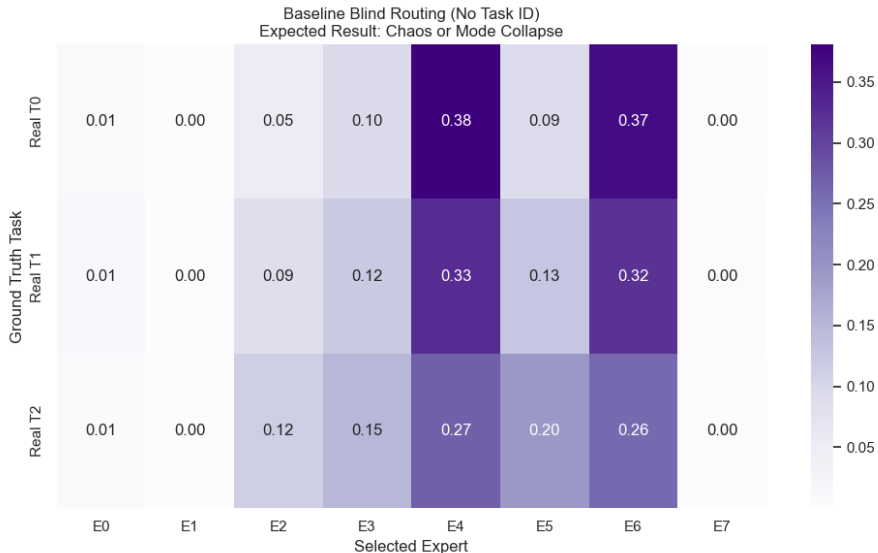


Figure 6: Routing distribution of the Standard MoE Baseline under blind inference.

4.3.3 Experiment III: The Necessity of Conflict (Pure Blind Baseline)

To rigorously verify whether the semantic emergence in CDSP relies on the conflict mechanism rather than merely data statistics, we introduce a Pure Blind Baseline. This model is trained entirely without Task IDs, relying solely on image content and auxiliary load-balancing losses. Since the training process is instruction-free, the inference behavior mirrors the training state; thus, we focus directly on the converged routing distribution at Epoch 9.

Semantic Entanglement and the Failure of Auxiliary Loss. Figure 7 illustrates the routing distribution of the Pure Blind Baseline. Unlike CDSP, which achieves clear separation, this baseline exhibits severe Semantic Entanglement:

- **Resource Contention:** Experts E0, E6, and E7 become "hotspot resources" shared indiscriminately by all tasks. The system gravitates towards a "Winner-Take-All" configuration dominated by these few experts.
- **Lack of Isolation:** Crucially, Task 2 (Fashion-MNIST, Objects) fails to isolate itself from the symbolic tasks. It directs 34% of its traffic to Expert E0 and 20% to Expert E6. Simultaneously, Task 0 (MNIST, Symbols) also relies heavily on E0 (24%) and E6 (28%). The overlap in expert utilization between distinct semantic categories (Symbols vs. Objects) indicates a failure to decouple features.
- **The "Pseudo-Balance" Trap:** While the auxiliary loss prevents single-expert collapse, it forces an "egalitarian" distribution where distinct tasks are coerced into sharing experts to satisfy statistical uniformity.

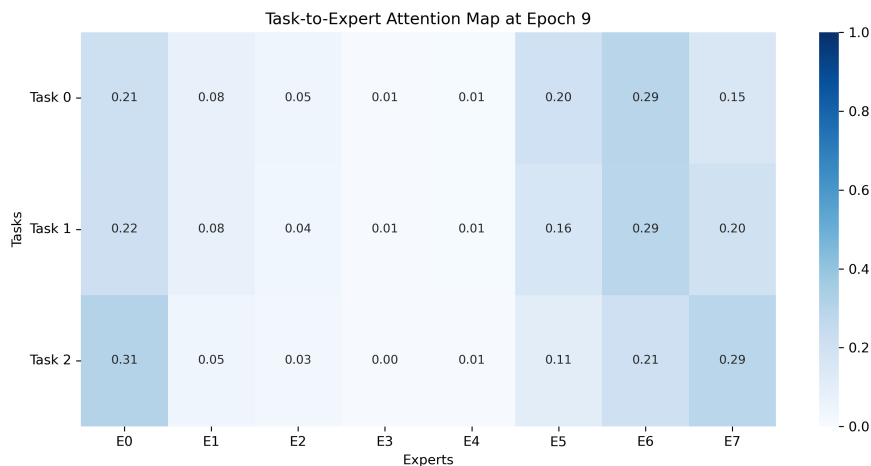


Figure 7: Routing distribution of the Pure Blind Baseline at Epoch 9.

Conclusion: Conflict as the Driver of Structure. Comparing Experiment I and III reveals the fundamental role of the conflict mechanism. Without the penalty for gradient interference, the model defaults to a "mixed sharing" strategy to minimize global loss, resulting in a chaotic overlap of symbolic and object features. The conflict game in CDSP is therefore identified as the essential force that breaks symmetry and drives the system toward modular disentanglement.

5 Conclusion

In this work, we challenged the prevailing design paradigm of Sparse Mixture-of-Experts, which relies on disjoint parameter storage and heuristic load-balancing constraints. We identified that such structural isolation, coupled with explicit task routing, leads to severe instruction overfitting and knowledge fragmentation. To address this, we introduced CDSP-MoE, a framework that grounds expert specialization in the physical interaction of gradients within a shared subspace.

Our contributions are threefold. First, by replacing static routing tables with a dynamic, conflict-driven pruning mechanism, we demonstrated that modularity can emerge purely from the minimization of physical interference. Second, our experiments revealed a critical trade-off: *CDSP-MoE initially lags behind the baseline in classification accuracy during early training*

phases. We interpret this as an *evolutionary tax*—while the baseline rapidly minimizes loss by memorizing simple ID-to-expert mappings ("shortcut learning"), CDSP-MoE must invest compute cycles to resolve gradient conflicts and restructure its topology. However, this initial cost yields a significant structural dividend: unlike the baseline which collapses under blind inference, CDSP-MoE evolves robust, content-aware routing pathways that disentangle symbolic concepts from object features without human supervision. Third, the comparison with the Pure Blind Baseline highlighted that auxiliary load-balancing losses alone are insufficient for semantic decoupling; the adversarial signal provided by the gradient conflict game is essential for breaking symmetry.

Limitations and Future Work. While CDSP-MoE offers a principled path toward autonomous modularity, it incurs a computational cost. Calculating the gradient conflict matrix requires storing lagged gradients, which increases memory overhead compared to standard forward-only gating. Additionally, our current validation is limited to vision classification tasks. Future work will focus on scaling this architecture to Large Language Models, investigating whether conflict-driven pruning can spontaneously separate distinct reasoning capabilities (e.g., coding vs. creative writing) and mitigate catastrophic forgetting in continuous learning scenarios. We believe that grounding neural architecture search in physical gradient dynamics represents a promising step toward interpretable and self-organizing artificial intelligence.

References

- [1] Damai Dai et al. Deepseek-moe: Towards ultimate expert specialization in mixture-of-experts language models. *arXiv preprint arXiv:2401.06066*, 2024.
- [2] William Fedus et al. Switch transformers: Scaling to trillion parameter models with simple and efficient sparsity. In *Advances in Neural Information Processing Systems (NeurIPS)*, 2021.
- [3] Alexandra Gessner et al. The universal weight subspace hypothesis. *arXiv preprint arXiv:2512.05117*, 2025.
- [4] Edward J. Hu et al. Lora: Low-rank adaptation of large language models. In *International Conference on Learning Representations*, 2022.
- [5] Dmitry Lepikhin et al. Gshard: Scaling giant models with conditional computation and automatic sharding. *arXiv preprint arXiv:2006.16668*, 2020.
- [6] Noam Shazeer et al. Outrageously large neural networks: The sparsely-gated mixture-of-experts layer. *arXiv preprint arXiv:1701.06538*, 2017.
- [7] Longrong Yang et al. Solving token gradient conflict in mixture-of-experts for large vision-language model. International Conference on Learning Representations (ICLR), 2025. ICLR 2025 Presentation.
- [8] Tianhe Yu et al. Gradient surgery for multi-task learning. In *Advances in Neural Information Processing Systems (NeurIPS)*, 2020.
- [9] Qingru Zhang, Min Chen, Alexander Bukharin, Pengcheng He, Yu Cheng, Weizhu Chen, and Tuo Zhao. Adalora: Adaptive budget allocation for parameter-efficient fine-tuning. In *ICLR*, 2023.
- [10] Yanqi Zhou et al. Mixture-of-experts with expert choice routing. *arXiv preprint arXiv:2202.09368*, 2022.

A Appendix

A.1 Detailed Hyperparameters

To ensure reproducibility, we list the detailed hyperparameters used for the CDSP-MoE experiments in Table A1.

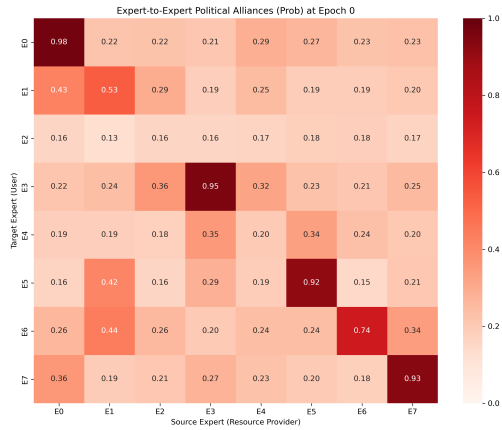
Table A1: Hyperparameter settings for the Heterogeneous Multi-Task Experiment.

Category	Hyperparameter	Value
Architecture	Logical Experts (N)	8
	Physical Base Dim (D_{base})	256
	Expert Subspace Rank (r)	32
	Hidden Size (D_{hidden})	256
Optimization	Optimizer	AdamW
	Base Learning Rate (η_{base})	5×10^{-3}
	Topology Learning Rate (η_{topo})	5×10^{-2} (10 \times)
	Weight Decay (Base)	1×10^{-2}
	Weight Decay (Topology)	0.0
	Batch Size	128
	Total Epochs	10
Loss Weights	λ_{task}	1.0
	$\lambda_{conflict}$	10.0
	$\lambda_{sparsity}$ (L1)	1×10^{-4}
Regularization	Task Dropout (p_{drop})	0.1

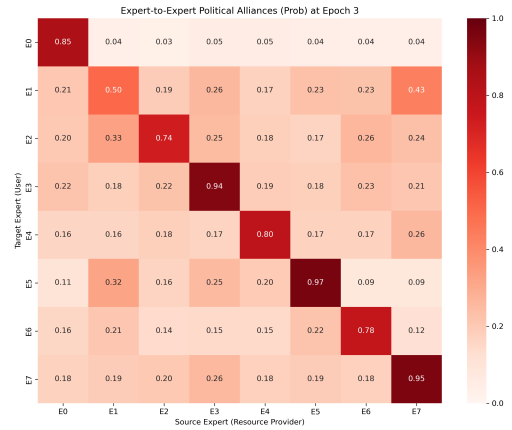
A.2 Supplementary Visualizations: The Evolution of Structure

To further illustrate the emergent properties of CDSP-MoE, we present the frame-by-frame evolution of the topology matrix and routing distribution.

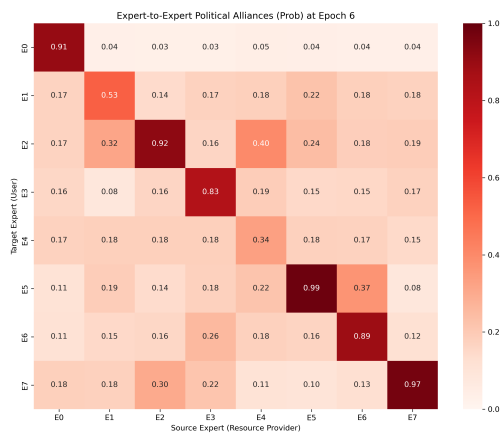
Topology Sparsification. Figure A1 displays the topology matrix $\sigma(\mathbf{A})$ at four distinct training stages. It clearly shows the transition from a dense, noisy initialization to a sparse, diagonal-dominant structure.



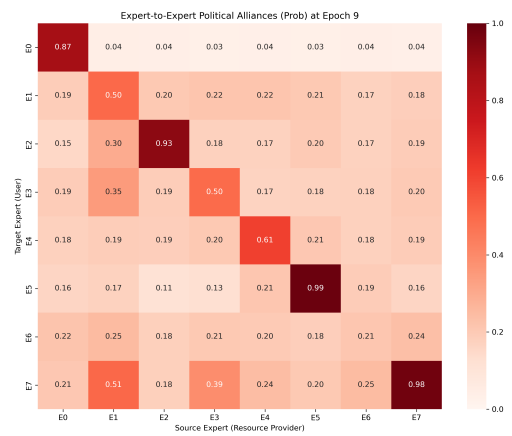
(a) Epoch 0: Initialization



(b) Epoch 3: Early Competition



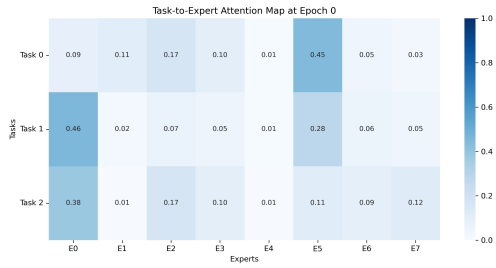
(c) Epoch 6: Pruning Phase



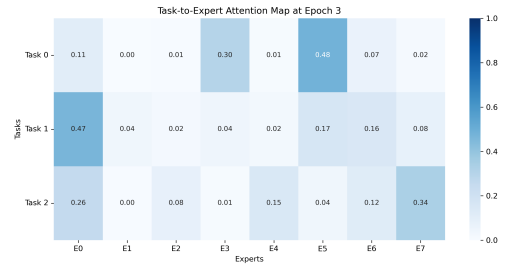
(d) Epoch 9: Final Convergence

Figure A1: Visualizing the progressive sparsification of the Topology Matrix $\sigma(\mathbf{A})$. Note how the "noise" connections (light blue) fade away, leaving only strong structural links (dark red).

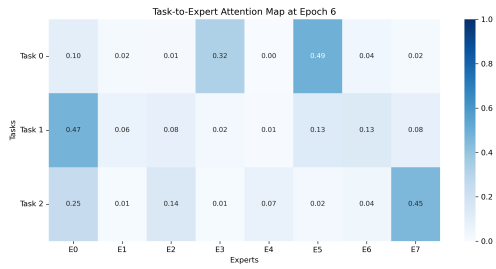
Routing Decision Boundary Shift. Figure A2 illustrates how the router's understanding of the tasks shifts over time. Initially (Epoch 0-3), the router struggles to differentiate KMNIST from FMNIST. By Epoch 6, the dedicated "Object Expert" (E7) begins to emerge, and by Epoch 9, the semantic separation is complete.



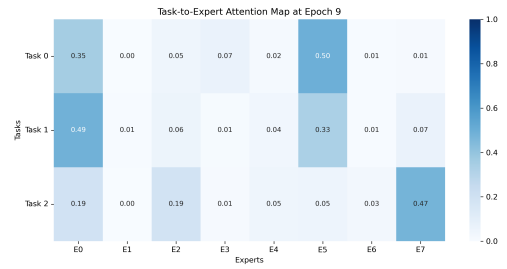
(a) Epoch 0: Random Assignment



(b) Epoch 3: Emerging Patterns



(c) Epoch 6: Semantic Separation



(d) Epoch 9: Stable Modularity

Figure A2: Evolution of Task Routing. The heatmaps show how the model gradually learns to group symbolic tasks (T0, T1) while isolating the object task (T2) to a specific expert.